

AperTO - Archivio Istituzionale Open Access dell'Università di Torino

**In vitro and in vivo effects of toceranib phosphate on canine osteosarcoma cell lines and xenograft orthotopic models**

**This is a pre print version of the following article:**

*Original Citation:*

*Availability:*

This version is available <http://hdl.handle.net/2318/1722333> since 2021-03-05T11:58:53Z

*Published version:*

DOI:10.1111/vco.12562

*Terms of use:*

Open Access

Anyone can freely access the full text of works made available as "Open Access". Works made available under a Creative Commons license can be used according to the terms and conditions of said license. Use of all other works requires consent of the right holder (author or publisher) if not exempted from copyright protection by the applicable law.

(Article begins on next page)



**In vitro and in vivo effects of toceranib phosphate in canine osteosarcoma cell lines and xenograft orthotopic models**

Journal:	<i>Veterinary and Comparative Oncology</i>
Manuscript ID	Draft
Manuscript Type:	Original Article
Keywords:	Tumor Biology, Tyrosine Kinase, Comparative Oncology, Mouse Models, In vitro Models
<p>Note: The following files were submitted by the author for peer review, but cannot be converted to PDF. You must view these files (e.g. movies) online.</p> <p>supplementary video 1.avi</p>	

SCHOLARONE™  
Manuscripts

## ***In vitro* and *in vivo* effects of toceranib phosphate in canine osteosarcoma cell lines and xenograft orthotopic models**

### **Abstract**

Canine osteosarcoma (OSA) is the most common primary malignant bone tumour with a high metastatic rate and poor prognosis. Toceranib phosphate (TOC) (Palladia®, Zoetis, U.S.A.) is a veterinary tyrosine kinase inhibitor (TKI) that selectively inhibits VEGFR-2, PDGFRs and c-Kit, but its efficacy in canine OSA is not fully understood. Here, we evaluated the functional effects of TOC on six OSA cell lines by transwell, wound healing and colony formation assays. Subsequently, two cell lines (Wall and Penny) were selected and inoculated in mice by intra-femur injection, developing an orthotopic xenograft model of canine OSA. For each cell line, 30 mice were injected, half of them used as control and the other half treated with TOC at 40 mg/kg body weight for 20 days; then mice were sacrificed and subjected to necroscopy. TOC inhibited cellular growth in all the cell lines and reduced invasion and migration in Penny and Wall cell lines. Significantly, TOC treatment decreased tumour growth only in mice inoculated with Penny. Moreover, specific transcripts of PDGFRs and c-Kit resulted down-regulated in these tumours. Immunohistochemical studies demonstrated a significant reduction of Ki67 in treated mice when compared to controls. Results obtained demonstrated that TOC is able to slightly inhibit cell growth *in vitro*, while its effect is evident only in Penny's xenograft model, where TOC significantly reduced tumour dimension and proliferating index without modifying apoptosis markers and mitotic index. These data may open a new scenario in canine OSA treatment and patient selection based on TKI targets expression.

## Introduction

Considering the high similarity at clinical, histopathological and molecular level, spontaneous tumours in dog are considered potential models for human diseases, representing an alternative to rodents for studying cancer biology and therapy<sup>1,2</sup>. Canine osteosarcoma (OSA) represents the most common primary malignant bone tumour, accounting for more than 80% of all bone tumours, being locally aggressive, and characterized by a high metastatic potential and poor prognosis<sup>1,3,4</sup>. Furthermore, the role of several tyrosine kinases receptors (TKRs) in the pathogenesis of canine OSA has recently been demonstrated<sup>5-7</sup>, as well as the opportunity to use tyrosine kinase inhibitors (TKI) against specific targets<sup>8,9</sup>.

TKI have radically changed the treatment approach and prognosis in several human tumours<sup>10,11</sup>; also in veterinary medicine this class of molecules resulted promising in few cancer histotypes<sup>12-15</sup>. Toceranib phosphate (TOC) (Palladia<sup>®</sup>, Zoetis, U.S.A) is a specific veterinary TKI that selectively inhibits VEGFR-2, PDGFRs and c-Kit and is currently approved for treatment of mast cell tumours<sup>16,17</sup>. However, there is increasing evidence that other solid tumours such as anal sac, head-neck and thyroid carcinomas, and OSA can be successfully treated with TOC<sup>18-19</sup>. Although, a recent clinical trial showed controversial results when using Palladia<sup>®</sup> as a single agent in canine metastatic OSA<sup>20</sup>.

Xenograft mouse models represent important tools to investigate the in vivo response to cancer therapeutic interventions. Previously published canine OSA mouse models were heterotopic and obtained implanting OSA cells intramuscularly (IM) or subcutaneously (SC)<sup>21-23</sup>, however intrinsic limitations were evident such as OSA cells were not exposed to the constitutive microenvironment. Consequently, the biological behaviour of the xenograft tumour and its response to therapy might have not completely reflected the disease progress. Orthotopic mouse models represent a more reliable

1  
2  
3 approach to evaluate tumour progression and pharmacological treatment efficacy. As  
4 mentioned previously, the clinical use of TOC in canine OSA is still scientifically argued  
5 and further investigations are needed. Considering the relevance of canine OSA both in  
6 veterinary medicine and comparative oncology, the aims of this study were to evaluate the  
7 functional effects of TOC in primary OSA cell lines and to develop orthotopic mice models  
8 of canine OSA. In addition, mRNA and protein changes of the preferential targets of TOC,  
9 as well as the clinical response, were also evaluated *in vivo*.

## 21 **Material and Methods**

### 23 *Cell lines and cell culture*

24  
25  
26 Seven primary canine OSA cell lines ("Penny", "Wall", "Desmond", "Sky", "Dark",  
27 "Lord" and "Pedro"), previously established by Maniscalco et al. (2013)<sup>6</sup>, were used in this  
28 study. All cell lines were maintained in Iscove's standard medium supplemented with 10%  
29 foetal bovine serum (FBS), 1% glutamine, 100 µg/mL penicillin and 100 µg/mL  
30 streptomycin, cultured at 37°C in a humidified atmosphere of 5% CO<sub>2</sub>, and passaged upon  
31 reaching confluence. A normal osteoblastic cell line (OSB) was isolated from a healthy dog  
32 using a procedure described before<sup>5</sup>.

### 42 *Transwell assay*

43  
44 The migration capability of the OSA cell lines was evaluated as follows. Cells were  
45 trypsinized, resuspended in Iscove's standard medium and counted in Bürker chambers.  
46 Subsequently, 1.5 X 10<sup>4</sup> cells were resuspended in 200 µl of supplemented Iscove's  
47 standard medium and added to the non-coated upper chamber of a transwell with 8 µm  
48 pore size filter (Corning Coster, Cambridge, MA, USA). To test the effects of TOC on the  
49 migratory capability of canine OSA cell lines, 800 µl of supplemented Iscove's standard  
50 medium with 1 µM of TOC was added to the lower chamber (treated groups) of the wells.

1  
2  
3 For controls, 800  $\mu$ l supplemented Iscove's standard medium without TOC was added.  
4  
5 After 48 hours incubation, cells on the upper side of the filter were mechanically removed  
6  
7 with a cotton swab, and both cells migrated to the lower side of the transwell and those  
8  
9 that reached the bottom of the wells were incubated with 5  $\mu$ g/mL Hoechst 33342 (Sigma  
10  
11 Diagnostic, St Louis, MO, USA) in 1 mL culture medium at 37°C under 5% CO<sub>2</sub> for 20  
12  
13 minutes, rinsed with PBS (Phosphate Buffer Solution) for 10 minutes 3 times. Both the  
14  
15 filter and the bottom of the wells were photographed with a fluorescent equipped  
16  
17 microscope at 100x and cells were counted using ImageJ software. Analysis was run in  
18  
19 triplicate.  
20  
21  
22

#### 23 24 *Wound healing assay*

25  
26 Considering the results obtained by transwell assay, Penny and Wall cell lines were  
27  
28 selected for the mobility assay. After trypsinization, 2 x 10<sup>5</sup> cells/well were plated in a 6-  
29  
30 wells plates to grow. When the confluence was reached, the monolayer was wounded by  
31  
32 applying a manual scratch and using a sterile 20  $\mu$ L pipette tip. The cellular debris was  
33  
34 removed with a gentle wash with complete medium and the supplemented Iscove's  
35  
36 medium with 1  $\mu$ M of TOC (treated groups) or without TOC (control groups) was added to  
37  
38 the cells. The ability of the cells to repair the wound was evaluated by real time microscopy  
39  
40 for 48 hours. Cell migration was monitored using a Leica AF6000 LX (Leica Microsystems,  
41  
42 Wetzlar, Germany) inverted microscope equipped with a Leica DFC350FX digital camera  
43  
44 and the photographs were taken every 30 minutes for 48 hours. The distance between two  
45  
46 parallel lines was measured in 5 different areas along the length of the wound and the  
47  
48 analysis was run in duplicate.  
49  
50  
51  
52

#### 53 54 *Colony formation assay*

55  
56 Penny and Wall were resuspended in 0.4% type VII low melting agarose in DMEM  
57  
58 (10% FBS) at 2 X 10<sup>4</sup> cells/well, plated on a layer of 0.8% agarose in Iscove's medium  
59  
60

(10% FBS) in 6-well culture plates and cultured at 37°C with 5% CO<sub>2</sub>. After 24 hours, the medium was removed and replenished with fresh medium with 1 µM of TOC (treated groups) or without TOC (control groups). The medium was changed every 3 days and after 3 weeks, colonies >100 µm and <100µm in diameter were counted with an inverted phase-contrast microscope. Colony formation assays were repeated in triplicates.

#### *Cell growth assay*

Penny and Wall cell lines were plated in 6-well plates and grown until 90% of confluence (highly proliferating), then detached and counted in a Bürker chamber. A total of 3000 cells were seeded in 6-well plates till attachment at a maximum of 6 hours, and TOC was added to the treated wells at 1µM concentration. After 72 hours, cells were rinsed with PBS and incubated with 5 µg/mL Hoechst 33342 (Sigma Diagnostic, St Louis, MO, USA) in 1 mL culture medium at 37 °C under 5% CO<sub>2</sub> for 20 minutes. Cells were then rinsed again with PBS, observed under a fluorescent microscope at 100x and nuclei were counted using ImageJ software.

#### *Orthotopic xenograft mouse model*

A total of 60 female *nu/nu* mice, 4–5 week-old, purchased by Charles River Laboratories (Calco, Milan) were housed under pathogen free condition with a 12h light/12h dark schedule, fed autoclaved standard chow and water *ad libitum*. Mice were manipulated and housed according to protocols approved by the XXX University Bioethical Committee and the Italian Ministry of Health (Authorization receipt n. 149401894128). For the intra-femur injections, exponentially growing cells (Penny and Wall) were harvested, counted and resuspended in PBS to a final concentration of 1 X 10<sup>7</sup> cells/ml. The animals were anesthetized with zolazepam/tiletamine (45 mg/kg) and xylazine (7.5 mg/kg). The knee of the mouse was fixed beyond 90° and 1 X 10<sup>6</sup> cells resuspended in 100 µl of PBS were injected into the distal femur using a 25-gauge needle. On day 0, 30 mice were

1  
2  
3 injected using Penny and Wall, respectively. Twice a week, mice were monitored to  
4  
5 determine the appearance and/or clinical signs of the engrafted tumour. When an average  
6  
7 tumour size of 0.5 cm in the largest diameter was obtained, daily treatment with TOC or  
8  
9 vehicle was initiated. Mice were randomly assigned into each group. According to  
10  
11 literature, mice were administered once daily with TOC at 40 mg/kg body weight in citrate  
12  
13 buffered (pH 3.5) solution <sup>24,25</sup> for 20 days by oral gavage using rigid dosing cannula.  
14  
15 Control mice were treated only with citrate buffered saline administered with the same  
16  
17 procedure. Tumour growth was evaluated twice a week by measuring the tumour size by a  
18  
19 caliper. Tumour length (L) and width (W) were measured to calculate tumour volume (V)  
20  
21 as follows:  $(L \times W^2)/2$ . Contextually, body weight was also measured. Five mice were not  
22  
23 inoculated and used as body weight control.  
24  
25  
26  
27

28 Mice were checked up to 20 days post-treatment or till animal endpoint criteria were  
29  
30 reached (ill thrift, visible lameness, pain or severe weight loss), then they were humanely  
31  
32 euthanized by an intravenous overdose injection of sodium pentobarbital. At post-mortem  
33  
34 examination the tumours were excised and cut into two pieces to be frozen in liquid  
35  
36 nitrogen for RNA extraction and fixed in 10% neutral buffered formalin for routine  
37  
38 histological exam and immunohistochemistry.  
39  
40  
41

#### 42 *RNA extraction and quantitative reverse transcription PCR (RT-qPCR) expression analysis*

43

44 Total RNA from all the OSA cell lines and OSB, as well as from engrafted tumours,  
45  
46 was extracted using 1ml of TRIReagent (Sigma-Aldrich) and any residual genomic DNA  
47  
48 was removed using a DNase I Recombinant RNase free kit (Roche, Mannheim,  
49  
50 Germany). RNA concentration was determined by spectrophotometry (BioPhotometer,  
51  
52 Eppendorf, Hamburg, Germany). The ratio of the optical densities measured at 260 and  
53  
54 280 nm was >1.9 for all RNA samples. cDNA was synthesized from 1 µg of total RNA by  
55  
56 RT High-Capacity cDNA Reverse Transcription Kit (Applied Biosystems, Foster City, CA,  
57  
58  
59  
60



USA), according to the manufacturer's protocol. To determine the relative amounts of specific PDGFR $\alpha$ , PDGFR $\beta$ , VEGFR2 and c-Kit transcripts, RT-qPCR was performed using the CFX Connect Real-Time PCR System (Bio-Rad, Hercules, CA, USA). Primers for target and reference genes were designed on *Canis Familiaris* GenBank messenger RNA (mRNA) sequences using Primer 3 Software (version 4.0). Oligonucleotides were designed to cross the exon/exon boundaries to minimize the amplification of contaminant genomic DNA and were analyzed using the IDT tool (available at <http://www.idtdna.com/scitools/scitools.aspx>) for hairpin structure and dimer formation. Primer specificity was verified with BLAST analysis against the genomic NCBI database. Multiple housekeeping genes were selected among 5 potential internal control mRNAs in the dog (HPRT, GAPDH, RP13a, RP18s and RP32) and on the basis of efficiency value GAPDH was selected as the most suitable for the purpose.

Supplementary Table 1 summarizes the primer information, sequences, gene accession number and amplicon sizes. Real-time PCR parameters were: cycle 1, 95°C for 30 s; cycle 2, 95°C for 10 s, 60°C for 30 s for 40 cycles. Gene Expression was calculated using the formula of  $2^{-\Delta\Delta Cq}$  (fold increase), where  $\Delta\Delta Cq = \Delta Cq$  (target) –  $\Delta Cq$  (control) and  $\Delta Cq$  is the Cq of the target gene subtracted from the Cq of the housekeeping gene.

#### *Histopathological and Immunohistochemical analysis*

Systemic organs and tumours obtained from mice were fixed in 10% buffered formalin for 24 hours. When needed, tumours were decalcified in 10% formic acid, and procedures for histological examination were applied. Also, several histological parameters were selected and scored (see Supplementary Table 2).

Immunohistochemistry (IHC) was performed on 4  $\mu$ m thick paraffin sections derived from OSA originated in mice using an automated immunostainer (DAKO). After blocking peroxidase activity and heat-induced antigen retrieval, sections were incubated with Ki67,

1  
2  
3 c-Kit and caspase 3 antibodies (see supplementary Table 3). Positive immunostaining for  
4  
5 Ki67 was determined by counting 1000 cells in 10 high power randomly-selected  
6  
7 neighbouring, non-overlapping fields. The number of Ki67-positive and negative cells was  
8  
9 assessed by image analysis using ImageJ freeware and the number of positive cells was  
10  
11 expressed as the percentage of positively stained cells in the total number of cells<sup>26</sup>.  
12  
13 Immunohistochemical evaluation of caspase 3 was carried out by taking images at x40  
14  
15 microscope objective from 10 random fields per tumour, to provide an average index of  
16  
17 caspase 3 positive cells<sup>27</sup>. For the IHC evaluation of c-Kit expression, the specimens were  
18  
19 scored according to both the percentage of positively stained tumour cells and their  
20  
21 immunostaining intensity<sup>28</sup>.  
22  
23  
24  
25

### 26 *Statistical analysis*

27  
28 IHC results were grouped into contingency tables and analyzed using Fisher's exact  
29  
30 test or X<sup>2</sup> test while q-PCR and *in vitro* data assays were analyzed using Student's t test.  
31  
32 Data were analyzed using MedCalc Statistical Software version 13.3 (MedCalc Software  
33  
34 bvba). A p value lower than 0.05 was considered statistically significant.  
35  
36  
37  
38  
39

## 40 **Results**

### 41 ***TOC inhibits OSA cell migration in vitro***

42  
43 The effect of TOC on OSA cells migration was assessed by transwell migration and  
44  
45 wound healing assays. All the canine OSA cell lines showed the ability to migrate through  
46  
47 the membrane and to attach to the lower side. Few cells detached and reached the bottom  
48  
49 of the wells. Conversely, TOC treatment reduced OSA cell migration to the bottom of the  
50  
51 membrane, within a range from 26.5±11.6% (Penny) to 88.1±1.1% (Sky; Fig. 1a).  
52  
53 Inhibition of cells attachment by TOC ranged from 32±0.9% (Wall) to 93±15.7% (Lady; Fig.  
54  
55 1b). Representative images of Hoescht stained nuclei in untreated controls and TOC  
56  
57  
58  
59  
60

1  
2  
3 treated cells are shown in Figure 1c. Wound healing assay showed a similar inhibitory  
4  
5 effect in TOC treated OS cell lines (Supplementary Video 1). The migration rate was  
6  
7 decreased to  $43.9 \pm 24.8\%$  in Penny (Fig. 2a) and  $71.0 \pm 14.3\%$  in Wall (Fig. 2b).  
8  
9 Considering these preliminary results, Penny and Wall were selected for the following *in*  
10  
11 *vitro* and *in vivo* experiments.  
12  
13

### 14 ***TOC inhibits cell growth and anchorage-independent OSA cell growth in vitro***

15  
16 To assess the growth effect of TOC, Penny and Wall were exposed to TOC for 72  
17  
18 hours. TOC treatment reduced cell growth by  $14.6 \pm 2.5\%$  and  $32.16 \pm 4.2\%$  in Penny and  
19  
20 Wall, respectively. To investigate OSA cells growth on anchorage-independent conditions,  
21  
22 a colony formation assay was performed. Both cell lines formed colonies when grown  
23  
24 resuspended in agarose, but TOC treatment in Penny and Wall slightly decreased colony  
25  
26 numbers compared to untreated cells (Fig. 3a). Thereby, when considering exclusively the  
27  
28 colonies  $>100 \mu\text{m}$  in diameter, TOC treatment showed a higher inhibition of colony  
29  
30 formation, with a reduction of  $37.7 \pm 8.0\%$  for Penny and  $85.7 \pm 12.0\%$  for Wall (Fig. 3b).  
31  
32  
33  
34

### 35 ***TOC reduces in vivo tumour growth only in Penny xenograft model***

36  
37 To evaluate the activity of TOC *in vivo*, we generated two orthotopic xenograft  
38  
39 mouse models using Penny and Wall. Both cell lines were tumorigenic and primary  
40  
41 tumours were macroscopically visible 18 days after injection in 85% of mice (n=51) with a  
42  
43 volume of approximately 3-4 mm<sup>3</sup>. TOC treatment was started at 22 days post-inoculation  
44  
45 and finished at day 42. The experimental design and the time lines of the treatment are  
46  
47 shown in Figure 4a. Six mice engrafted with Penny (20%) and 3 mice engrafted with Wall  
48  
49 (10%) didn't develop tumours at any time, also confirmed at necropsy. Drug-related side  
50  
51 effects were observed after 3-4 days of treatment including dermatitis in 5 (33.3%) and 4  
52  
53 (26.7%) mice inoculated with Penny and Wall, respectively. However, TOC significantly  
54  
55 decreased tumour growth in mice inoculated with Penny, but not with Wall cell line (Fig.  
56  
57  
58  
59  
60

1  
2  
3 4b). Also, no differences in body weight between the four different groups were evident  
4  
5 (Fig. 4c).  
6

7  
8 ***TOC treatment reduces PDGFR $\alpha$ , PDGFR $\beta$ , VEGFR2 and c-Kit mRNA expression in***  
9  
10 ***both in vivo and in vitro models***

11  
12 Quantitative RT-PCR results (Fig. 5a) revealed that all the OSA cell lines had a  
13  
14 higher mRNA expression of both PDGFR $\alpha$  and PDGFR $\beta$  compared to the OSB control cell  
15  
16 line (P<0,05). The only exception was Dark cell line for PDGFR $\alpha$ . VEGFR2 and c-Kit  
17  
18 mRNAs were increased in 3 out of 7 OS cell lines (Penny, Wall and Lord) when compared  
19  
20 to the OSB cell lines (P<0,05). Finally, we examined PDGFR $\alpha$ , PDGFR $\beta$ , VEGFR2 and c-  
21  
22 Kit mRNA expression in tumours obtained from TOC treated and control mice. A  
23  
24 significant down regulation of PDGFR $\alpha$ , PDGFR $\beta$  and c-Kit in mice inoculated with Penny  
25  
26 and treated with TOC compared to controls was found, confirming *in vitro* results (Fig. 5b),  
27  
28 whereas no differences were retrieved in mice inoculated with Wall (Fig. 5b).  
29  
30  
31

32  
33 ***TOC treatment influences tumour cell density and KI-67 score***

34  
35 Histological examination of the xenograft tumors confirmed a chondroblastic OSA  
36  
37 from Penny (Fig. 6A) and osteoblastic productive OSA (Fig. 6B) from Wall<sup>7</sup>. No  
38  
39 differences for anisocytosis, anisokaryosis, presence of haemorrhages, vascular invasion,  
40  
41 bone marrow invasion or muscular invasion were found after treatment. Notably, the grade  
42  
43 of anisocytosis and anisokaryosis was always elevated (Fig. 6C) in association with  
44  
45 necrotic-haemorrhagic areas (Fig. 6D). Conversely, bone marrow invasion occurred in  
46  
47 12/51 tumours (23%) (Fig. 6E); muscular invasion in 48/51 samples (93%) (Fig. 6F), but  
48  
49 no differences were found between the two groups. Of note, in the only mouse of the study  
50  
51 (belonging to the Wall control group) in which vascular invasion was diagnosed, presence  
52  
53 of lung metastasis was also observed (Fig.6G).  
54  
55  
56  
57  
58  
59  
60

1  
2  
3 Histologically, TOC-treated Penny and Wall xenograft models had a decrease of tumour  
4 cell density when compared to vehicle-treated animals ( $p=0.015$  and  $p=0.03$ , respectively).  
5  
6 Although the differences were not significant, a trend towards a decrease in the amount of  
7 matrix and necrosis was observed after TOC treatment both in tumours originated from  
8 Penny and Wall. By immunohistochemistry, tumours from TOC treated mice showed a  
9 lower Ki-67 score (Fig.6H) when compared to tumours grown in vehicle-treated mice  
10 (Fig.6I). Also, a significant reduction of cellular density was obtained both in Penny and  
11 Wall engrafted tumours ( $p<0.005$ ). Conversely, Caspase 3 expression was not influenced  
12 by TOC treatment.  
13  
14  
15  
16  
17  
18  
19  
20  
21  
22  
23  
24  
25

## 26 Discussion

27  
28 OSA represents the most common primary malignant bone tumour in dog, with a  
29 high metastatic potential and poor prognosis<sup>1,29</sup>. In humans, this disease is still scarcely  
30 curable with a high rate of metastasis.<sup>30,31</sup> Comparative oncology studies have shown  
31 many similarities between OSA occurring in human and canine patients, and also in  
32 veterinary oncology the development of xenograft models<sup>32</sup> in mice represents nowadays  
33 an important alternative to investigate the microenvironment and the molecular  
34 mechanisms driving cancer growth, as well as to evaluate the biological effects of novel  
35 therapeutic agents such as TKIs.  
36  
37  
38  
39  
40  
41  
42  
43  
44  
45

46 In our study, we developed an orthotopic model of canine OSA and further tested  
47 the biological and pharmacological effects of TOC. To identify the most promising cell line,  
48 TKRs targets of TOC were firstly evaluated by RT-qPCR in seven canine OS cell lines. All  
49 of them showed an heterogenous amount of mRNA that was gene dependent.  
50 Interestingly, similar variations were previously described when considering protein<sup>6,33,34</sup>.  
51  
52  
53  
54  
55  
56  
57  
58  
59  
60

1  
2  
3 Cell lines were further investigated by several biological assays in order to  
4 determine whether cell migration was affected by treatment with TOC. Transwell assay  
5 demonstrated that all the OSA cell lines were able to migrate in absence of chemo-  
6 attractive factors; conversely migration was negatively affected by TOC, although to a  
7 different extent among cell lines. Interestingly, Penny and Dark resulted the most sensitive  
8 to TOC treatment using the proliferating assay, while the migration score was the highest  
9 in Penny and the lowest in Wall. Wound healing migration rate, colony formation and cell  
10 growth rate in soft agar assays revealed that both Penny and Wall were negatively  
11 affected by TOC treatment. Overall, these *in vitro* results suggested that Wall and Penny  
12 responded to TOC treatment by slightly reducing their migration and proliferating  
13 behaviour. This might be due to the ability of TOC to inhibit the kinase activity of the target  
14 receptors and consequently the downstream activated pathways, as demonstrated in  
15 previous results obtained by other authors where AG1296 induced down regulation of p-  
16 AKT in time and dose dependence<sup>6,35,36</sup>.

17  
18 To validate the *in vitro* results, both Penny and Wall cell lines were inoculated in an  
19 orthotopic model, and the cellular growth of OSA was monitored. Results demonstrated  
20 that both Penny and Wall cells were highly tumorigenic, showing engraftment after 18  
21 days. Also, tumour histology confirmed that both cell lines conserved the original  
22 morphological features. Interestingly, TOC treatment decreased the tumour growth in mice  
23 inoculated with Penny but not with Wall. Regarding the selected histological parameters,  
24 tumour cell density was reduced in treated mice compared to control mice independently  
25 from the cell line origin. It is worth noting that vascular invasion as well as lung metastasis  
26 was reported only in one mouse from Wall control group. This observation, even with  
27 several limitations, suggests a possible inhibitory effect on the metastatic spread by TOC  
28 as shown in the metastatic DARK cell line that resulted more sensitive to the TOC

1  
2  
3 treatment. Unfortunately, this observation cannot be confirmed statistically due to the low  
4  
5 number of occurrences. With regard to this aspect, it could be speculated that the  
6  
7 metastatic process is mediated by the microenvironment that develops within the  
8  
9 orthotopic model and that possibly depends on VEGFR2 expression, as recently  
10  
11 demonstrated in human OSA<sup>37</sup>. No mRNA expression modifications for PDGFRs,  
12  
13 VEGFR2 and c-Kit were found in tumours removed from control *versus* TOC-treated mice,  
14  
15 implying that TOC treatment did not act at the transcriptional level of these genes.  
16  
17

18  
19 Ki67 results demonstrated a lower proliferation index (PI) in TOC treated tumours  
20  
21 than in the ones of control mice (in both Penny and Wall groups). This data indicate a TOC  
22  
23 effect in decreasing tumour proliferation, but not on cell apoptosis, as shown by caspase-3  
24  
25 results. Interestingly, Sunitinib (SU11248) is the equivalent of TOC in humans being  
26  
27 administered in patients with gastrointestinal stromal tumours (GIST), neuroendocrine  
28  
29 tumours and renal carcinomas, while is off-label in human OSA<sup>38</sup> and recently it was  
30  
31 tested in xenograft models of human OSA cell lines showing an evident reduction of the  
32  
33 tumour growth and PI, thereby mimicking our results<sup>39</sup>.  
34  
35

36  
37 Today, clear indications for using TOC in canine OS treatment are not available,  
38  
39 and recent clinical trials do not support the use of TOC as a single agent therapy for  
40  
41 canine metastatic OS<sup>20,40</sup>. Moreover, the use of TOC in c-Kit mutated mast cell tumours  
42  
43 was also recently discussed<sup>41</sup>. Our results demonstrate that TOC is able to inhibit cell  
44  
45 growth *in vitro* only mildly, while its effect is more relevant in xenograft models.  
46  
47 Considering the relevant expression of PDGFRs, c-Kit and VEGFR2 in Penny, these data  
48  
49 suggest that TOC treatment might be more effective in tumours expressing these targets.  
50  
51 Further studies are needed to test the efficacy of this molecule in canine OSA, but these  
52  
53 results open a new scenario where only a subset of OS having high target levels might  
54  
55 respond to TOC treatment.  
56  
57  
58  
59  
60

## Bibliografia

1. Morello E, Martano M, Buracco P. Biology, diagnosis and treatment of canine appendicular osteosarcoma: Similarities and differences with human osteosarcoma. *Veterinary Journal*. 2011;189(3):268-277.
2. Withrow SJ, Powers BE, Straw RC, Wilkins RM. COMPARATIVE ASPECTS OF OSTEOSARCOMA - DOG VERSUS MAN. *Clinical Orthopaedics and Related Research*. 1991(270):159-168.
3. Farese JP, Kirpensteijn J, Kik M, et al. Biologic Behavior and Clinical Outcome of 25 Dogs with Canine Appendicular Chondrosarcoma Treated by Amputation: A Veterinary Society of Surgical Oncology Retrospective Study. *Veterinary Surgery*. 2009;38(8):914-919.
4. Casteleyn C, Sleeckx N, De Spiegelaere W, Heindryckx F, Coulon S, Van Steenkiste C. New therapeutic targets in veterinary oncology: Man and dog definitely are best friends. *Veterinary Journal*. 2013;195(1):6-7.
5. De Maria R, Miretti S, Iussich S, et al. met oncogene activation qualifies spontaneous canine osteosarcoma as a suitable pre-clinical model of human osteosarcoma. *J Pathol*. 2009;218(3):399-408.
6. Maniscalco L, Iussich S, Morello E, et al. PDGFs and PDGFRs in canine osteosarcoma: New targets for innovative therapeutic strategies in comparative oncology. *Veterinary Journal*. 2013;195(1):41-47.
7. Maniscalco L, Iussich S, Morello E, et al. Increased expression of insulin-like growth factor-1 receptor is correlated with worse survival in canine appendicular osteosarcoma. *Vet J*. 2015;205(2):272-280.
8. Mantovani FB, Morrison JA, Mutsaers AJ. Effects of epidermal growth factor receptor kinase inhibition on radiation response in canine osteosarcoma cells. *BMC Vet Res*. 2016;12:82.
9. Fahey CE, Milner RJ, Kow K, Bacon NJ, Salute ME. Apoptotic effects of the tyrosine kinase inhibitor, masitinib mesylate, on canine osteosarcoma cells. *Anticancer Drugs*. 2013;24(5):519-526.
10. Hojjat-Farsangi M. Small-molecule inhibitors of the receptor tyrosine kinases: promising tools for targeted cancer therapies. *Int J Mol Sci*. 2014;15(8):13768-13801.
11. Wu P, Nielsen TE, Clausen MH. FDA-approved small-molecule kinase inhibitors. *Trends Pharmacol Sci*. 2015;36(7):422-439.
12. Downing S, Chien MB, Kass PH, Moore PE, London CA. Prevalence and importance of internal tandem duplications in exons 11 and 12 of c-kit in mast cell tumors of dogs. *Am J Vet Res*. 2002;63(12):1718-1723.
13. Amagai Y, Tanaka A, Matsuda A, et al. Heterogeneity of internal tandem duplications in the c-kit of dogs with multiple mast cell tumours. *J Small Anim Pract*. 2013;54(7):377-380.
14. London CA. Small molecule inhibitors in veterinary oncology practice. *Vet Clin North Am Small Anim Pract*. 2014;44(5):893-908.
15. London CA. Tyrosine kinase inhibitors in veterinary medicine. *Top Companion Anim Med*. 2009;24(3):106-112.
16. Robat C, London C, Bunting L, et al. Safety evaluation of combination vinblastine and toceranib phosphate (Palladia(R)) in dogs: a phase I dose-finding study. *Vet Comp Oncol*. 2012;10(3):174-183.
17. London CA, Malpas PB, Wood-Follis SL, et al. Multi-center, placebo-controlled, double-blind, randomized study of oral toceranib phosphate (SU11654), a receptor tyrosine kinase inhibitor, for the treatment of dogs with recurrent (either local or distant) mast cell tumor following surgical excision. *Clin Cancer Res*. 2009;15(11):3856-3865.
18. London C, Mathie T, Stingle N, et al. Preliminary evidence for biologic activity of toceranib phosphate (Palladia((R))) in solid tumours. *Vet Comp Oncol*. 2012;10(3):194-205.
19. Gardner HL, London CA, Portela RA, et al. Maintenance therapy with toceranib following doxorubicin-based chemotherapy for canine splenic hemangiosarcoma. *BMC Vet Res*. 2015;11:131.



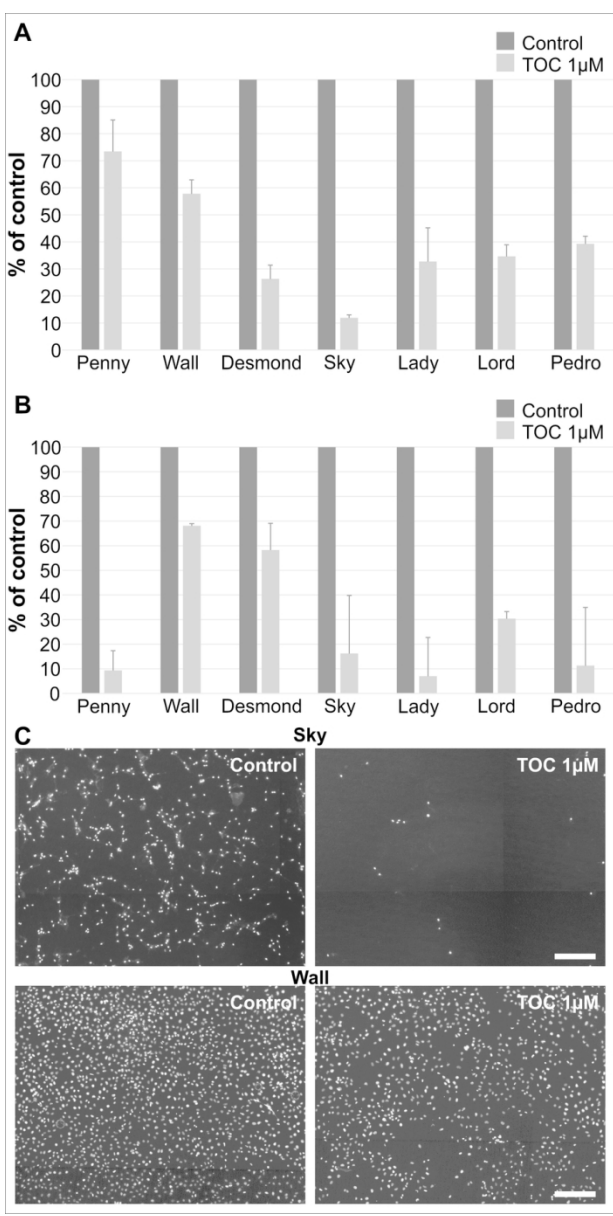
1  
2  
3  
4  
5  
6  
7  
8  
9  
10  
11  
12  
13  
14  
15  
16  
17  
18  
19  
20  
21  
22  
23  
24  
25  
26  
27  
28  
29  
30  
31  
32  
33  
34  
35  
36  
37  
38  
39  
40  
41  
42  
43  
44  
45  
46  
47  
48  
49  
50  
51  
52  
53  
54  
55  
56  
57  
58  
59  
60

20. Laver T, London CA, Vail DM, Biller BJ, Coy J, Thamm DH. Prospective evaluation of toceranib phosphate in metastatic canine osteosarcoma. *Vet Comp Oncol*. 2017.
21. Coomer AR, Farese JP, Milner R, et al. Development of an intramuscular xenograft model of canine osteosarcoma in mice for evaluation of the effects of radiation therapy. *Am J Vet Res*. 2009;70(1):127-133.
22. Farese JP, Fox LE, Detrisac CJ, Van Gilder JM, Roberts SL, Baldwin JM. Effect of thalidomide on growth and metastasis of canine osteosarcoma cells after xenotransplantation in athymic mice. *Am J Vet Res*. 2004;65(5):659-664.
23. Hong SH, Kadosawa T, Mochizuki M, Matsunaga S, Nishimura R, Sasaki N. Effect of all-trans and 9-cis retinoic acid on growth and metastasis of xenotransplanted canine osteosarcoma cells in athymic mice. *Am J Vet Res*. 2000;61(10):1241-1244.
24. London CA, Hannah AL, Zadovoskaya R, et al. Phase I dose-escalating study of SU11654, a small molecule receptor tyrosine kinase inhibitor, in dogs with spontaneous malignancies. *Clin Cancer Res*. 2003;9(7):2755-2768.
25. Mendel DB, Laird AD, Xin X, et al. In vivo antitumor activity of SU11248, a novel tyrosine kinase inhibitor targeting vascular endothelial growth factor and platelet-derived growth factor receptors: determination of a pharmacokinetic/pharmacodynamic relationship. *Clin Cancer Res*. 2003;9(1):327-337.
26. Dolka I, Sapierzynski R, Krol M. Retrospective study and immunohistochemical analysis of canine mammary sarcomas. *BMC Vet Res*. 2013;9:248.
27. McCleese JK, Bear MD, Fossey SL, et al. The novel HSP90 inhibitor STA-1474 exhibits biologic activity against osteosarcoma cell lines. *Int J Cancer*. 2009;125(12):2792-2801.
28. Mijji LN, Petrilli AS, Di Cesare S, et al. C-kit expression in human osteosarcoma and in vitro assays. *Int J Clin Exp Pathol*. 2011;4(8):775-781.
29. Morello E, Martano M, Buracco P. Biology, diagnosis and treatment of canine appendicular osteosarcoma: similarities and differences with human osteosarcoma. *Vet J*. 2011;189(3):268-277.
30. Ferguson WS, Goorin AM. Current treatment of osteosarcoma. *Cancer Invest*. 2001;19(3):292-315.
31. Vormoor B, Knizia HK, Batey MA, et al. Development of a preclinical orthotopic xenograft model of ewing sarcoma and other human malignant bone disease using advanced in vivo imaging. *PLoS One*. 2014;9(1):e85128.
32. Guan G, Lu Y, Zhu X, et al. CXCR4-targeted near-infrared imaging allows detection of orthotopic and metastatic human osteosarcoma in a mouse model. *Sci Rep*. 2015;5:15244.
33. Maniscalco L, Iussich S, Morello E, et al. Increased expression of insulin-like growth factor-1 receptor is correlated with worse survival in canine appendicular osteosarcoma. *Veterinary Journal*. 2015;205(2):272-280.
34. Gattino F, Maniscalco L, Iussich S, et al. PDGFR-alpha, PDGFR-beta, VEGFR-2 and CD117 expression in canine mammary tumours and evaluation of the in vitro effects of toceranib phosphate in neoplastic mammary cell lines. *Vet Rec*. 2018.
35. Yancey MF, Merritt DA, Lesman SP, Boucher JF, Michels GM. Pharmacokinetic properties of toceranib phosphate (Palladia, SU11654), a novel tyrosine kinase inhibitor, in laboratory dogs and dogs with mast cell tumors. *J Vet Pharmacol Ther*. 2010;33(2):162-171.
36. Halsey CH, Gustafson DL, Rose BJ, et al. Development of an in vitro model of acquired resistance to toceranib phosphate (Palladia(R)) in canine mast cell tumor. *BMC Vet Res*. 2014;10:105.
37. Zheng B, Ren T, Huang Y, Guo W. Apatinib inhibits migration and invasion as well as PD-L1 expression in osteosarcoma by targeting STAT3. *Biochem Biophys Res Commun*. 2018;495(2):1695-1701.
38. Demetri GD, van Oosterom AT, Garrett CR, et al. Efficacy and safety of sunitinib in patients with advanced gastrointestinal stromal tumour after failure of imatinib: a randomised controlled trial. *Lancet*. 2006;368(9544):1329-1338.

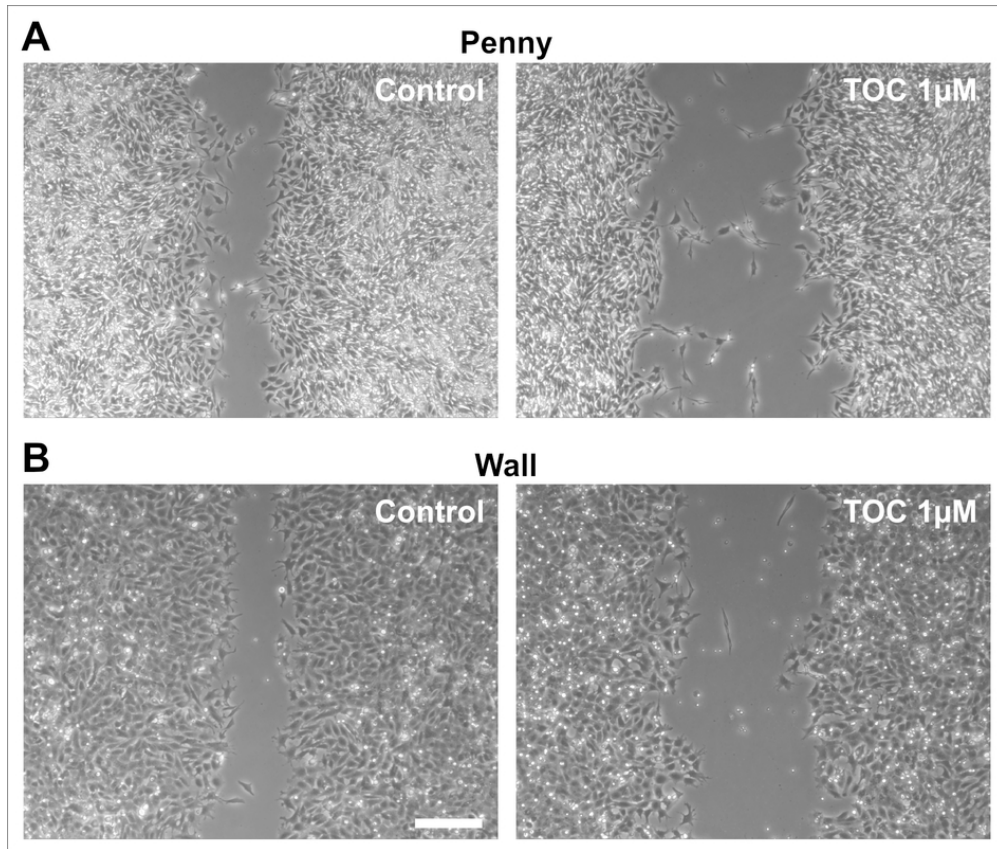
- 1  
2  
3 39. Kumar RM, Arlt MJ, Kuzmanov A, Born W, Fuchs B. Sunitinib malate (SU-11248) reduces tumour  
4 burden and lung metastasis in an intratibial human xenograft osteosarcoma mouse model. *Am J*  
5 *Cancer Res.* 2015;5(7):2156-2168.  
6  
7 40. Laver T, London CA, Vail DM, Biller BJ, Coy J, Thamm DH. Prospective evaluation of toceranib  
8 phosphate in metastatic canine osteosarcoma. *Vet Comp Oncol.* 2018;16(1):E23-e29.  
9  
10 41. Weishaar KM, Ehrhart EJ, Avery AC, et al. c-Kit Mutation and Localization Status as Response  
11 Predictors in Mast Cell Tumors in Dogs Treated with Prednisone and Toceranib or Vinblastine. *J Vet*  
12 *Intern Med.* 2018;32(1):394-405.  
13  
14  
15  
16  
17  
18  
19  
20  
21  
22  
23  
24  
25  
26  
27  
28  
29  
30  
31  
32  
33  
34  
35  
36  
37  
38  
39  
40  
41  
42  
43  
44  
45  
46  
47  
48  
49  
50  
51  
52  
53  
54  
55  
56  
57  
58  
59  
60

For Peer Review Only

1  
2  
3  
4  
5  
6  
7  
8  
9  
10  
11  
12  
13  
14  
15  
16  
17  
18  
19  
20  
21  
22  
23  
24  
25  
26  
27  
28  
29  
30  
31  
32  
33  
34  
35  
36  
37  
38  
39  
40  
41  
42  
43  
44  
45  
46  
47  
48  
49  
50  
51  
52  
53  
54  
55  
56  
57  
58  
59  
60

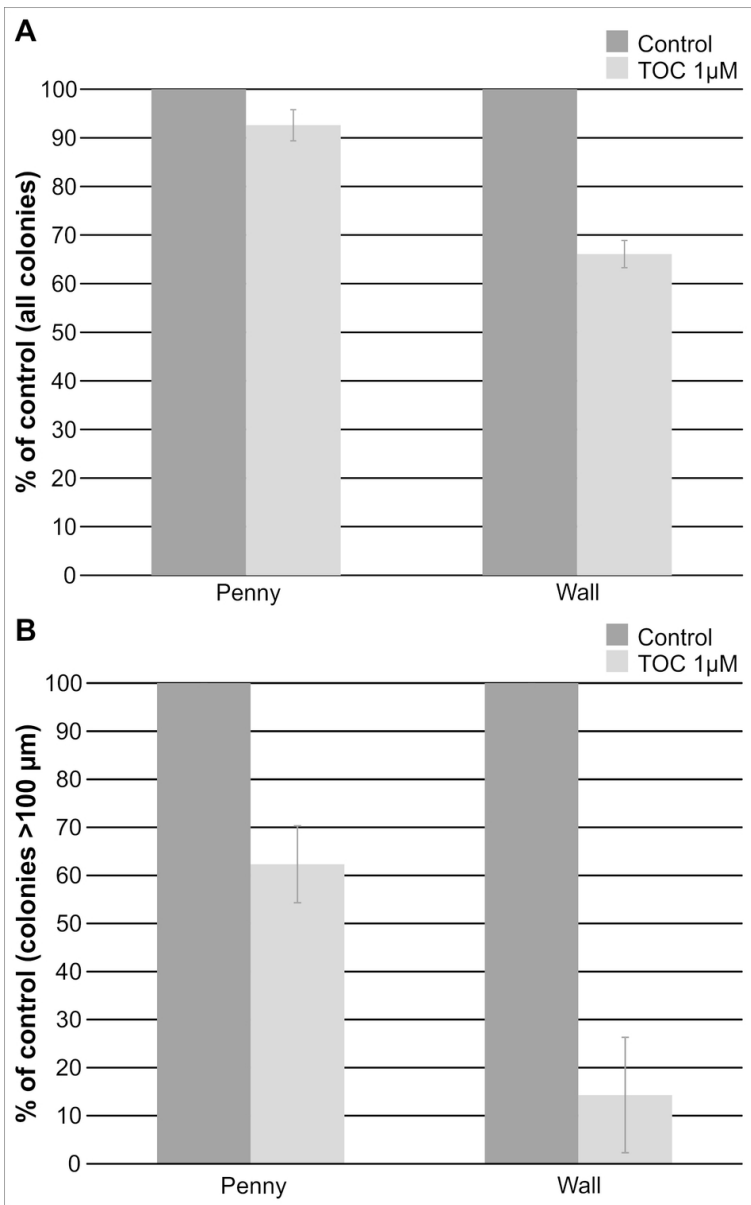


80x156mm (300 x 300 DPI)

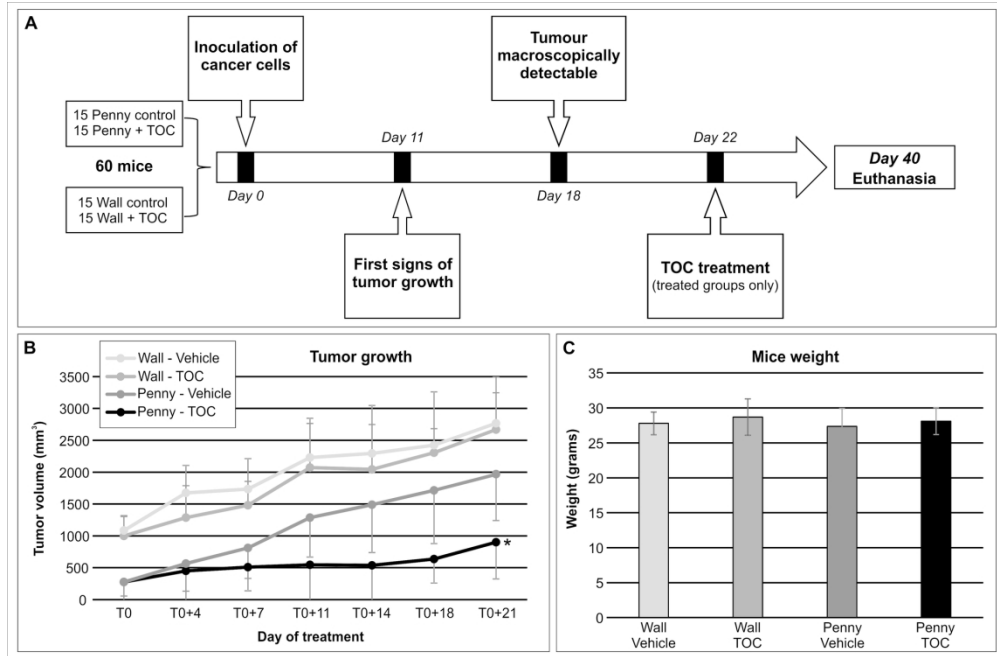


80x67mm (300 x 300 DPI)

1  
2  
3  
4  
5  
6  
7  
8  
9  
10  
11  
12  
13  
14  
15  
16  
17  
18  
19  
20  
21  
22  
23  
24  
25  
26  
27  
28  
29  
30  
31  
32  
33  
34  
35  
36  
37  
38  
39  
40  
41  
42  
43  
44  
45  
46  
47  
48  
49  
50  
51  
52  
53  
54  
55  
56  
57  
58  
59  
60

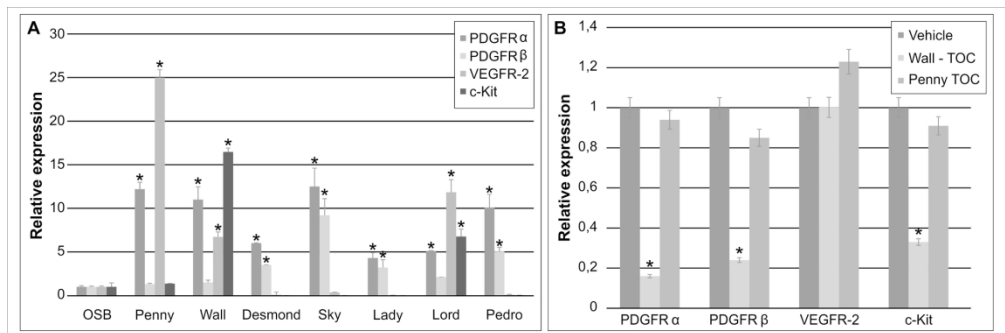


80x127mm (300 x 300 DPI)

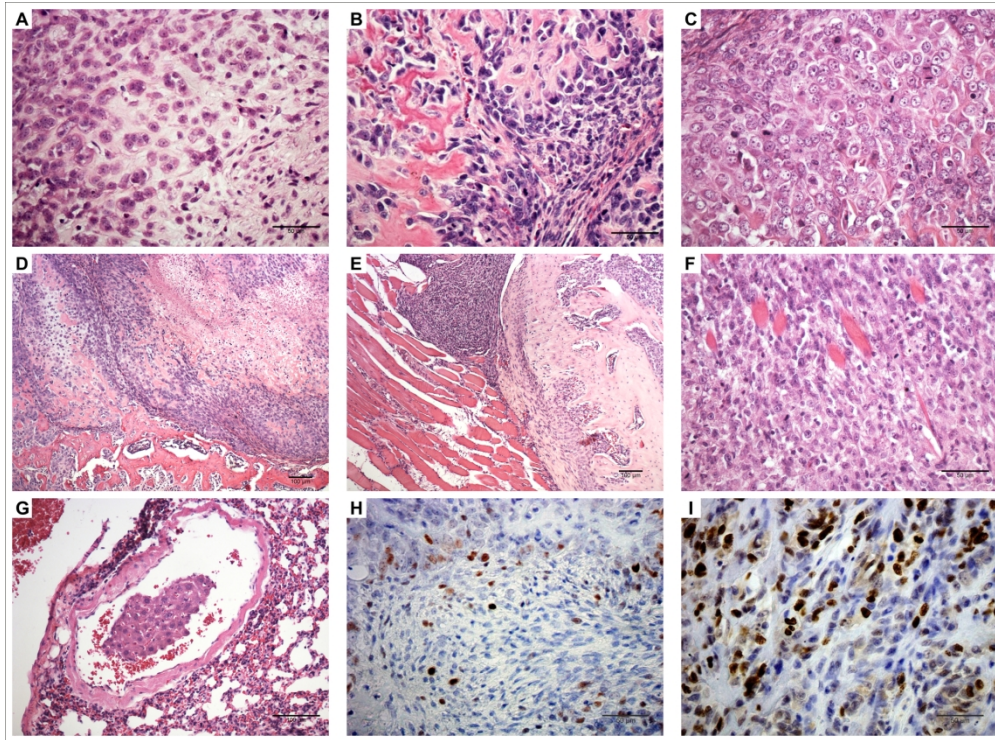


180x118mm (300 x 300 DPI)

1  
2  
3  
4  
5  
6  
7  
8  
9  
10  
11  
12  
13  
14  
15  
16  
17  
18  
19  
20  
21  
22  
23  
24  
25  
26  
27  
28  
29  
30  
31  
32  
33  
34  
35  
36  
37  
38  
39  
40  
41  
42  
43  
44  
45  
46  
47  
48  
49  
50  
51  
52  
53  
54  
55  
56  
57  
58  
59  
60



180x59mm (300 x 300 DPI)



180x133mm (300 x 300 DPI)



## LEGENDS TO FIGURES

### Figure 1.

Cellular migration by transwell assay. (A) Percentage of cells attached to the lower side of the membrane and (B) the bottom of the lower chamber in all canine OSA cell lines treated with Toceranib (1 $\mu$ M) compared to the control (untreated). Error bars represent standard deviation of experimental triplicates. (C) Immunofluorescence assay showing cells migrated to the bottom of the lower chamber in Sky and Wall cell lines treated with TOC compared to the untreated cell lines (Hoescht staining) (200x, Scale bar= 250 $\mu$ m).

### Figure 2.

Wound Healing Migration Assay. Penny cell line (A) and Wall cell line (B) after 48h of treatment with TOC (1  $\mu$ M) with respectively not treated cell lines. (400x, Scale bar= 100 $\mu$ m).

### Figure 3.

Colony Formation Assay. (A) Percentage of colonies formed in agarose in Penny and Wall cell lines treated with TOC 1 $\mu$ M compared to the untreated cells. (B) Percentage of colonies (>100 $\mu$ m diameter) formed in agarose in Penny and Wall cell lines treated with TOC 1 $\mu$ M. Error bars represent standard deviation of experimental triplicates.

### Figure 4.

Experimental Xenograft Design. (A) Experimental timeline of OSA xenograft on mice and TOC treatment. (B) Measurements of tumour volume of xenografts of Wall or Penny cell lines in mice, along the treatment with TOC and with a vehicle (from T0 to T0+21days). As shown in the figure mice inoculated with Penny cells and treated with TOC showed a significant smaller tumour volume compared to those treated with a vehicle (\*p<0.05). (C) Weight of mice with Wall or Penny xenografts, treated with TOC or with vehicle, at the end of the experiment. No variation between the groups is highlighted.

### Figure 5.

Quantitative PCR. (A) Expression of PDGFR- $\alpha$ , PDGFR- $\beta$ , VEGFR-2 and c-Kit transcripts in primary osteosarcoma (OSA) cell lines. PDGFR- $\alpha$  mRNA were expressed at higher levels in 7/7 OSA cell lines, PDGFR- $\beta$  in 4/7, VEGFR-A transcript had a higher expression

1  
2  
3 in 4/7 OSA cell lines and c-Kit in 2/7, compared to the normal cell line (OSB) (\*p<0.05).  
4 The fold increase of each specific mRNA was normalised with normal OSB cell line and  
5 the error bars indicate the standard deviation of experimental triplicates. (B) Expression by  
6 quantitative PCR of PDGFR- $\alpha$ , PDGFR- $\beta$ , VEGFR-2 and c-Kit in primary Wall and Penny  
7 OS cell lines treated with TOC, compared to the control (untreated). Wall cell line showed  
8 a lower expression of PDGFR- $\alpha$ , PDGFR- $\beta$  and c-Kit when treated (\*p<0.05). Penny cell  
9 did not show any significant variation. The fold increase of each specific mRNA was  
10 normalised with the control cell line and the error bars indicate the standard deviation of  
11 experimental triplicates.  
12  
13  
14  
15  
16  
17  
18

19 Figure 6.

20  
21 Histological features of osteosarcoma xenografts. (A) Penny cell line xenograft showing  
22 chondroblastic. Neoplastic cells have a chondrocyte-like morphology and are located  
23 within lacunae. H&E stain (400x, bar= 50  $\mu$ m). (B) Wall cell line xenograft showing,  
24 osteoblastic hystotype Neoplastic cells surrounded by irregular trabeculae of osteoid  
25 matrix. H&E stain (400x, bar= 50  $\mu$ m) and (C) Marked anisocytosis and anisokaryosis. (D)  
26 Necrosis involving the 30% of the neoplastic tissue. (200x, scale bar= 100 $\mu$ m). (E) Bone  
27 marrow invasion (200x, scale bar= 100 $\mu$ m). (F) Muscular invasion (200x, scale bar=  
28 100 $\mu$ m). (G) Pulmonary Metastasis (200x, scale bar= 100 $\mu$ m). Nuclear Ki-67  
29 immunolabelling respectively in Penny xenograft (H) treated with TOC and not treated  
30 mice (I). Streptavidin–biotin–peroxidase method. Mayer's haematoxylin counterstain  
31 (400x, bar= 50  $\mu$ m).  
32  
33  
34  
35  
36  
37  
38  
39  
40  
41  
42  
43  
44  
45  
46  
47  
48  
49  
50  
51  
52  
53  
54  
55  
56  
57  
58  
59  
60

**Supplementary Table 1.**

Primer sequences employed in q-PCR

Primer	Gene	Sequence
Forward	VEGFR-2	5'-CATGCACGGTCTACGCCGTCC-3'
Reverse	VEGFR-2	5'-CAGCTTGGGCGGGCTTGTAGG-3'
Forward	CD117	5'-CTCGCGGCGCCTGGGATTTT-3'
Reverse	CD117	5'-GAAGAGCCTGTCCGGACGCC-3'
Forward	PDGFR- $\alpha$	5'-CATCCCCCTGCCCGACATCG-3'
Reverse	PDGFR- $\alpha$	5'-TGAGCTGTGTCTGTTCTTCTTGCC-3'
Forward	PDGFR- $\beta$	5'-GTCCTCAAAGGCCAGGCACTGTGG-3'
Reverse	PDGFR- $\beta$	5'-CCCCGGGGGTGTGATGACCAG-3'
Forward	GAPDH	5'-GGCACAGTCAAGGCTGAGAAC-3'
Reverse	GAPDH	5'-CCAGCATCACCCATTGAT-3'

**Supplementary Table 2.**

Histological parameters and scores for histological examination of tumours xenograft

PARAMETER	
Anisokaryosis and anisocytosis <sup>1</sup>	0= no variation 1= mild variation 2= moderate variation 3= marked variation
Tumour cell density <sup>2</sup>	1= <25% of cells 2= 25-50% of cells 3= 50-75% of cells 4= >75% of cells
Mitotic Index <sup>1</sup>	Number of mitosis in 10 high-power fields (400x)
Amount of matrix <sup>2</sup>	1= >50% matrix 2= 25-50% matrix 3= <25% matrix
Amount of necrosis <sup>1</sup>	0= no necrosis 1= <25% of necrosis 2= 15-50% of necrosis 3= >59% of necrosis
Haemorrhage	0= absence of haemorrhage 1= presence of haemorrhage
Invasion of the bone	0= absence of invasion 1= bone invasion
Invasion of the bone marrow	0= absence of invasion 1= bone marrow invasion
Invasion of the muscle	0= absence of invasion 1= muscle invasion

1. Kruse MA, Holmes ES, Balko JA, Fernandez S, Brown DC, Goldschmidt MH. Evaluation of clinical and histopathologic prognostic factors for survival in canine osteosarcoma of the extracranial flat and irregular bones. *Vet Pathol.* 2013;50(4):704-708.
2. Kirpensteijn J, Kik M, Rutteman GR, Teske E. Prognostic significance of a new histologic grading system for canine osteosarcoma. *Vet Pathol.* 2002;39(2):240-246.

1  
2  
3  
4  
5  
6  
7  
8  
9  
10  
11  
12  
13  
14  
15  
16  
17  
18  
19  
20  
21  
22  
23  
24  
25  
26  
27  
28  
29  
30  
31  
32  
33  
34  
35  
36  
37  
38  
39  
40  
41  
42  
43  
44  
45  
46

**Table 1.**  
Antibodies used in immunohistochemistry

<b>Antibody</b>	<b>Type</b>	<b>Source</b>	<b>Concentration</b>
Ki67	Mouse monoclonal	Dako, Burlingame, CA, USA	1:75
Caspase-3	Rabbit polyclonal	R&D systems, Minneapolis, MN, USA	1:250
c-Kit	Rabbit polyclonal	Dako, Burlingame, CA, USA	1:750

For Peer Review Only